Optimal Sensing/Actuation Strategies for Vibration and Acoustic Control of Optical Systems

Suk-Min Moon*
Department of Mechanical Engineering and Materials Science
Duke University, Durham, NC 27708 USA.

Leslie P. Fowler †
CSA Engineering, Inc., 1600 Eubank Blvd., SE, Albuquerque, NM 87123, USA.

Robert L. Clark‡
Department of Mechanical Engineering and Materials Science
Duke University, Durham, NC 27708 USA.

Optical jitter can result in the beam pointing inaccuracy and poor optical system performance. With a correlated measurement of the disturbance, improved control performance can be achieved. In this research, an adaptive optimal sensing strategy for optical systems is proposed. When an array of reference sensors is available, an optimal set of reference sensors that are coupled to modes of interests can be selected. The weighted reference signal from the optimal sensor set is then used in an adaptive control design algorithm. An adaptive generalized predictive control design algorithm combined with the proposed adaptive optimal sensing strategy achieves better performance than the control system using only one of the reference sensors. The overall algorithm is also advantageous in the presence of time-varying or uncertain disturbances. The proposed technique is applied to an experimental test bed in which multiple accelerometer sensors measure the structural vibration of optical elements. Reduction of the structural vibration of optical components is attained using a fast steering mirror which results in a reduction of the corresponding jitter.

Nomenclature

α_i, η_i	Linear model parameters for the optimization
$\hat{\alpha}_i$, $\hat{\beta}_i$, $\hat{\gamma}_i$	Linear model parameters for control design
γ_i	Hankel Singular Values for i^{th} mode of the system
$d(t)$	Reference sensor signal
$d_w(t)$	Weighted reference sensor signal
$\mathbf{B}$, $\mathbf{C}$	Input and output matrices of the state-space model
p	Number of parameters in the model estimation algorithm
P	Number of parameters in the control design
$u(t)$	Control input
$y(t)$	Error sensor output

*Research Assistant, E-mail: minmoon@duke.edu
†PE: Senior Engineer, CSA Engineering, Inc. E-mail: leslie.fowler@csaengineering.com
‡Professor, E-mail: rclark@duke.edu

Report Documentation Page

Form Approved
OMB No. 0704-0188

1. REPORT DATE	2. REPORT TYPE	3. DATES COVERED
2005		**00-00-2005 to 00-00-2005**

4. TITLE AND SUBTITLE	5a. CONTRACT NUMBER
Optimal Sensing/Actuation Strategies for Vibration and Acoustic Control of Optical Systems	5b. GRANT NUMBER
	5c. PROGRAM ELEMENT NUMBER
6. AUTHOR(S)	5d. PROJECT NUMBER
	5e. TASK NUMBER
	5f. WORK UNIT NUMBER
7. PERFORMING ORGANIZATION NAME(S) AND ADDRESS(ES) **CSA Engineering,1451 Innovation Parkway SE Suite 100,Albuquerque,NM,87123**	8. PERFORMING ORGANIZATION REPORT NUMBER
9. SPONSORING/MONITORING AGENCY NAME(S) AND ADDRESS(ES)	10. SPONSOR/MONITOR'S ACRONYM(S)
	11. SPONSOR/MONITOR'S REPORT NUMBER(S)

12. DISTRIBUTION/AVAILABILITY STATEMENT
Approved for public release; distribution unlimited

13. SUPPLEMENTARY NOTES
The original document contains color images.

14. ABSTRACT
see report

15. SUBJECT TERMS

16. SECURITY CLASSIFICATION OF:			17. LIMITATION OF ABSTRACT	18. NUMBER OF PAGES	19a. NAME OF RESPONSIBLE PERSON
a. REPORT **unclassified**	b. ABSTRACT **unclassified**	c. THIS PAGE **unclassified**		**12**	

I. Introduction

Jitter, the deviation of a light beam from its intended path, results in beam pointing inaccuracy and poor optical system performance. Jitter is caused by vibrations of optical elements and their mounting supports.[1] Hence, it becomes a topic of consideration for optical applications such as semiconductor equipment manufacturing, data storage equipment and vehicle-borne optical systems.[2–5]

Active control using secondary sources to suppress jitter shows promise particularly at low frequencies where structural and acoustic motions are well defined.[1,6–9] Adaptive feedforward control algorithms have also demonstrated jitter reduction in the presence of time-varying disturbances.[5,10] The performance of an adaptive feedforward control system is however dependent on a measure of the disturbance. Since the jitter is caused by correlated as well as uncorrelated sources of noise and vibration propagating through multiple mechanical and acoustic paths, the disturbance measurement coherent with the jitter measurement is important.[11,12]

In this research, an optimal sensor weighting technique is proposed.[13] When multiple reference sensors are available to measure the disturbances, the coupling to the targeted mode(s) is scored for an array of reference sensor sets. The weighted reference sensor signal from an optimal sensor set is used in the adaptive control design. The overall algorithm is demonstrated on the jitter test bed using electromagnetic actuators to disturb the optical elements.

II. Control problem formulation

Figure 1 shows the block diagram considered in this research.[13] There exists an exogenous disturbance and it disturbs a plant which is either a model or an actual system such as an optical system. In a plant, there is a secondary actuator such as a fast steering mirror to reduce the vibrations caused by the disturbance. Vibration measurement sensors are available in the plant and sensors are used for the error measurement or reference measurement. The overall control objective is to minimize some norm, for example the H_2 norm, of the transfer function from disturbance ω to error sensor y. The proposed strategy is:

1) Select an optimal set of reference sensors and their weighting by a means to rank the reference sensor sets based on the ability to couple well to the targeted mode(s) for control, and thereby feed through the weighted sensor signal to a control design algorithm.

2) Design a feedback and feedforward controller using the error sensor signal and the weighted reference sensor signal.

3) Perform all processes in real-time so that it could respond to environmental and system changes.

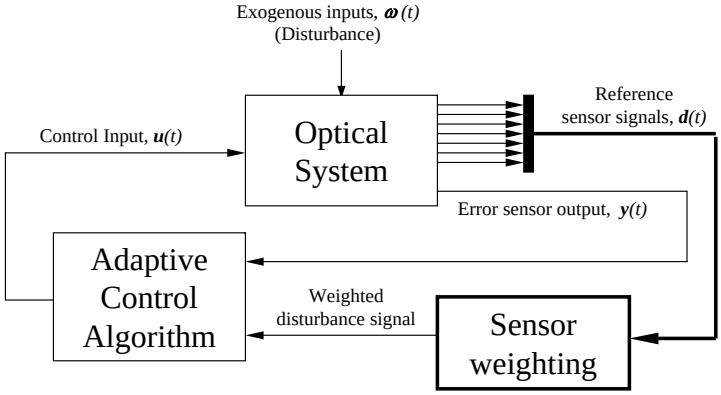

Figure 1. Overall block diagram

III. Model Identification

A recursive least-squares (RLS) identification algorithm is applied to estimate a linear relationship between an error sensor and reference sensors.[14] One property of the RLS algorithm is that it allows us to omit some data during operation. In the discrete-time application, for instance, if the data sampling rate is too fast to perform all computations in a data sampling period, the recursion can be applied in a slower sampling rate. This is because the recursion does not rely on the relation between two successive data histories.

The RLS algorithm estimates a set of linear model parameters recursively:

$$y(t) = \sum_{i=1}^{p} \alpha_i y(t-i) + \sum_{i=0}^{p} \eta_i \nu(t-i) \tag{1}$$

where $y(t)$ is the error sensor output, $\nu(t) = [u(t) \quad d(t)]^T$, and $u(t)$ and $d(t)$ are the control input signal and reference sensor signal, respectively. Note that Equation (1) describes the linear relationships between the error sensor signal as output and the reference sensor signal as an extra input in addition to the control input signal. The coefficients, α_i and η_i, are the model parameters to be estimated using the RLS algorithm, and the details can be found in many references.[13,15,16]

IV. Optimal Sensor Weighting Algorithm

For a given linear model, the next step is to rank reference sensor sets and select a set that is coupled effectively to modes of interest. In order to find an optimal set of sensors and their weighting, the optimization needs to rank sensor sets as well as converge on an optimal solution based on these rankings. The sets are ranked through a previously developed process involving the application of Hankel Singular Value (HSV) approximation.[17,18] The optimization was accomplished through the use of the genetic algorithm.

A. Sensor scoring metric

The basis for the modal coupling scoring metric lies in approximating the Hankel Singular Values (HSVs) corresponding to system modes for the input/output path of interest.[13,17,18] An approximation of the squared HSVs for the i^{th} mode of the system, γ_i^4, can be written as

$$\gamma_i^4 \approx \frac{\mathrm{tr}[\mathbf{B}_i \mathbf{B}_i^T]\mathrm{tr}[\mathbf{C}_i \mathbf{C}_i^T]}{16\delta_i^2} \tag{2}$$

$$\delta = \zeta \omega_n \tag{3}$$

where $\mathbf{B}_i$ and $\mathbf{C}_i$ terms are the input and output matrices respectively from the state-space model corresponding to the i^{th} mode and δ_i is the real part of the natural logarithm of the i^{th} eigenvalue. The state-space model is obtained from a linear model, given in Equation (1), using the Eigensystem Realization Algorithm (ERA).[14] The scoring metric was previously described in references,[17,18] and will not be repeated here.

B. Genetic optimization

The optimization algorithm is designed to converge on an optimal solution through a series of iterations of mating based on the beneficial ranking of the pairs.[19] The definition of an individual set is defined by two parameters – sensor combination and weighting of each sensor. These parameter vectors are then converted into a binary matrix of sixteen-digit resolution. A random starting population is constructed prior to implementation of the algorithm. Mating is determined based on a binary crossover strategy. Mutations are performed by allowing random adjustments to individual binary digits over a prescribed percentage of the mating events. A general diagram of the procedure is outlined in Figure 2.

In addition, an adjustment is made to retain the highest scoring set for the next iteration.[20] This adjustment forces the winner of each successive iteration to be at least as good as the previous one. This technique consistently yields similar results regardless of the parameters of the original population.

The resulting best set of reference sensors and their gains after a series of iterations is used to compute the weighted reference sensor signal which is coupled well to the targeted modes. The weighted reference sensor signal is then used in adaptive control design algorithm.

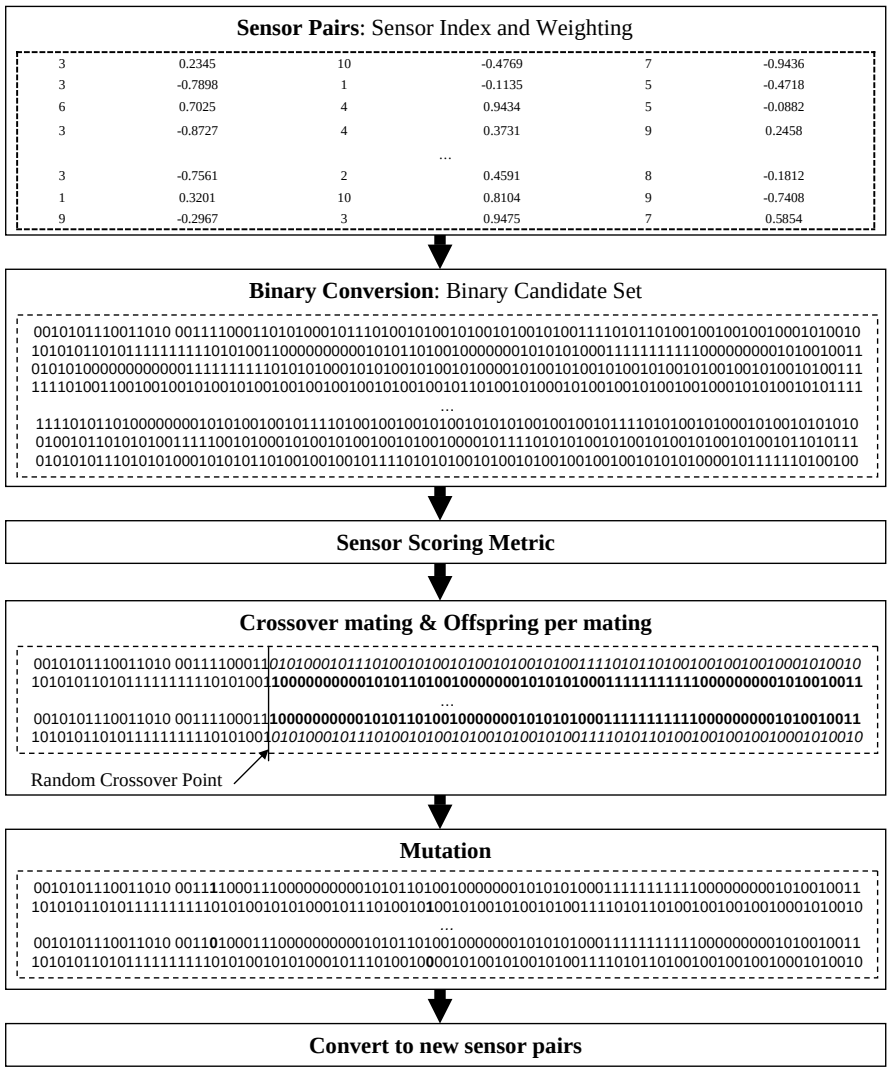

Figure 2. Diagram of genetic algorithm process

V. Adaptive Control Design

The adaptive generalized predictive control algorithm that combines the process of system identification and the process of generalized predictive control design are applied in the experimental demonstration.[5,21] Using the weighted reference sensor signal, $d_w(t)$, consider the deterministic model

$$y(t) = \sum_{i=1}^{P} \hat{\alpha}_i y(t-i) + \sum_{i=1}^{P} \hat{\beta}_i u(t-i) + \sum_{i=1}^{P} \hat{\gamma}_i d_w(t-i) \tag{4}$$

where $\hat{\alpha}_i$, $\hat{\beta}_i$, and $\hat{\gamma}_i$ are parameters of a model that represents the linear relationship between the error sensor signal, $y(t)$, and control input signal, $u(t)$, with the weighted reference signal, $d_w(t)$. The hat accent ($\hat{}$) is used to distinguish it from the model parameters in Equation (1). The subscript w is also used to distinguish it from the reference sensor signal, $d(t)$, in Equation (1). The model parameters in Equation (4) are obtained recursively using the RLS system identification algorithm in the same manner as summarized in Section III.

In the discrete time application, the process of GPC design can be applied in a slower sampling rate than the system identification process since the control gains are estimated indirectly. The indirect algorithm is a

straightforward implementation in which model parameters are estimated and the controller is designed from model parameters, while the direct algorithm estimates the controller parameters directly from measured and known data sets. In case of a slower sampling rate for the control design, it must be assumed that the system parameters do not change significantly. The controller is thus fixed until a new controller is computed and updated.

VI. Experimental demonstration

As shown in Figure 1, the overall algorithm can be divided into two processes: the process of the reference sensor weighting and the process of controller design. The sensor weighting algorithm performs the model estimation, the optimization, and the computation of the weighted reference signal. The adaptive generalized predictive control design is then performed based on the weighted reference sensor signal.

A. Experimental test bed

Experiments are performed with the optical jitter suppression test bed, illustrated in Figure 3. An Edmund 5mW Uniphase Helium-Neon cylindrical laser and an On-Trak Photonics 10 mm dual axis position sensing detector (PSD) are mounted on the one optical bench (see Figure 3(b)) and a fast steering mirror (FSM) is mounted on the other optical bench (see Figure 3(c).) A flat turning mirror and its mounting post are mounted on the 3 feet by 5 feet and 1/8 inch thick aluminum plate (see Figure 3(d).) A laser shines a beam on the turning flat mirror, reflects off of the FSM, and shines on the PSD. The aluminum plate is bolted down to a wooden frame and placed on a lab table to match the height with other optical benches. In addition to the optical components on the plate, CSA Engineering SA-1 actuators and PCB Piezotronics accelerometer sensors are mounted onto the aluminum plate. The CSA SA-1 actuators are used to disturb the plate and the vibration of the plate in the vertical direction becomes the critical source of jitter on the optical elements — a flat turning mirror and its post. The total number of 7 PCB Piezotronics accelerometer sensors are used to measure the plate vibration, and the PSD provides an optical measure of the structurally induced jitter. The locations of accelerometers, actuators, and the mounting post on the plate are shown in Figure 4.

Each accelerometer is connected to the PCB sensor signal conditioner and a 4^{th}-order Butterworth filter circuit with the cutoff frequency set to be 1 kHz. An Ithaco 24 dB/octave highpass filter, set to a cutoff frequency of 10 Hz, is used to remove the DC offset in the PSD signal to prevent the static position of the laser from saturating the $\pm$ 10 V A/D channels on the DSP board.

B. Experimental setup

The overall algorithm is implemented for real-time application using MATLAB/Simulink and the interface between the MATLAB/Simulink model and I/O boards(s) is performed using xPC Target and Real-Time Workshop (RTW.) It is an environment in which a desktop computer serving as a host PC generates executable code using Real-Time Workshop and a C/C++ compiler, and xPC Target downloads the executable code to a second PC acting as a target PC, which runs an application model in real time.

In the experimental demonstration, the overall algorithm is performed using two digital signal processing (DSP) platforms. First, the reference sensor weighting process is performed with a pair of a target and host computer — the target computer has a Pentium III 800 MHz processor and 384 megabyte (MB) memory and the host computer has a Pentium III 550 MHz processor and 384 MB memory. A National Instrument PCI-6024E I/O board is connected to a target computer. Second, the control design process is performed with another pair of a target and host computer — the target computer has an AMD 1.4 GHz processor and 512 MB memory and is connected to an UEI PD2 MFS I/O board.

The application algorithm loaded on each DSP platform is shown in Figure 5. The RLS system identification algorithm is loaded to the xPC Target PC and executed in real time. The xPC host PC connected with the xPC target PC through network performs the optimization process and updates an optimal set of reference sensors. Due to the time delay in the data transfer between the Target PC and the Host PC and computational complexity of the optimization process, the optimal set of sensor is fixed until a new set is computed and updated. The weighted reference sensor signal is then computed from the optimal set of reference sensors, and applied to the second xPC target PC in the same sample rate as data acquisition of error sensor.

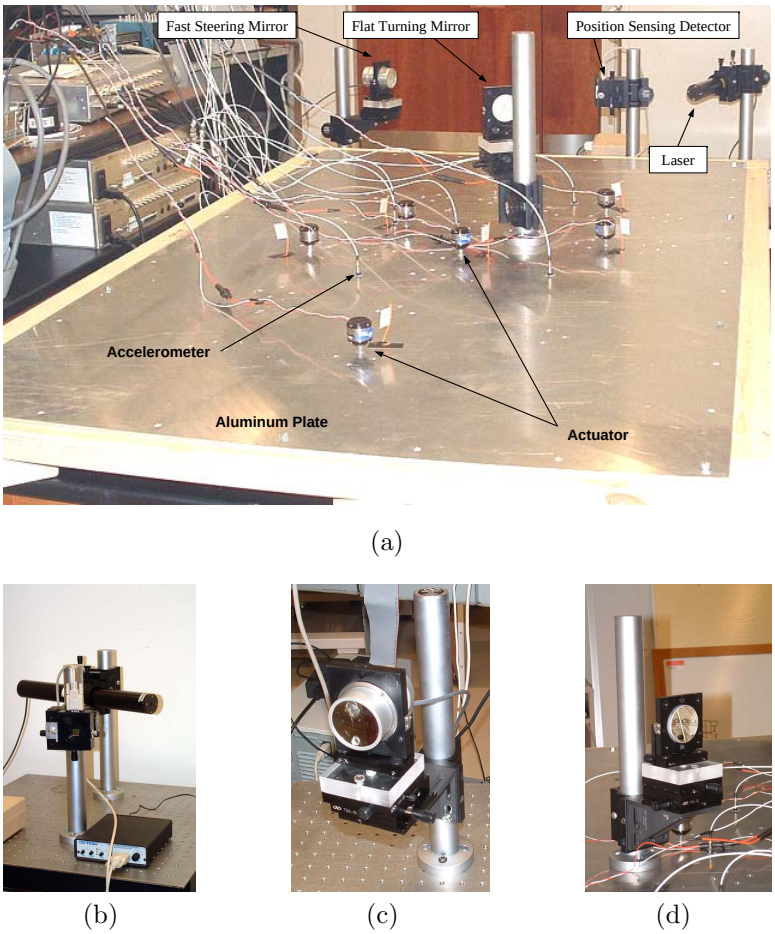

Figure 3. Experimental test bed: (a) Overall picture of experimental test bed, (b) Fast steering mirror, (c) Flat turning mirror and its post on the plate, (d) Laser and position sensing detector

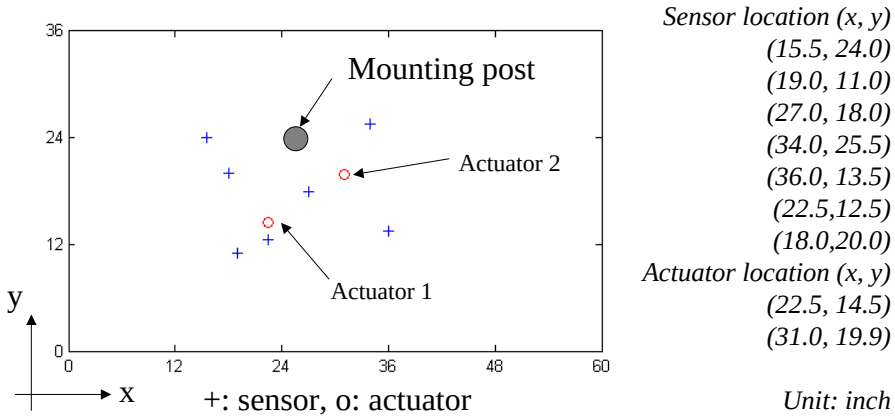

Figure 4. Location of accelerometers, actuators, and the mounting post on the plate

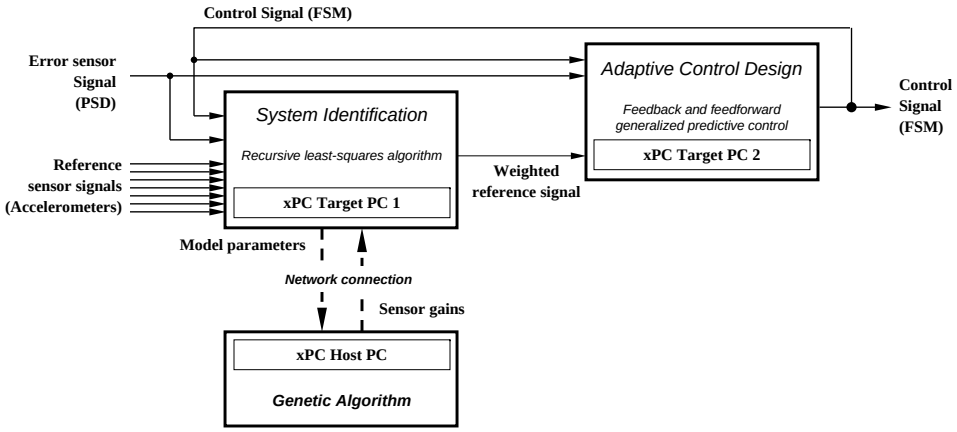

Figure 5. Algorithm on DSP platform

Prior to the application of the proposed algorithm, a band-limited (2 kHz) random disturbance signal was applied to one of the actuators mounted on the plate and the vibration response is measured from seven accelerometer sensors using a Siglab spectrum analyzer. Figure 6(a) shows the frequency response plot of the averaged magnitude of all accelerometers and Figure 6(b) shows the averaged magnitude squared coherence estimation plot between the disturbance signal and accelerometer signals. The coherence is a normalized cross-spectral density function of two time series — the stored signal to actuator and the measured signal from accelerometer.[25] As seen in Figure 6(b), a coherence near 0 dB is measured above 300 Hz. With this observation, the selection vector for the desirably coupled modes is chosen such that it includes all the modes between 300 Hz and 800 Hz of an identified model. The selection vector for the detrimental modal coupling is chosen to include all the modes below 300 Hz.[13]

C. Experimental Results

First, the overall algorithm is applied when the plate structure is disturbed by a sinusoidal wave. An actuator — actuator 2 in Figure 4 — is excited with single-frequency (550 Hz) sine wave. The error sensor signal from the PSD and the reference sensor signals from accelerometers are acquired at 2 kHz. The control input to the FSM is computed at 2 kHz. Due to the sample rate limit by the target PC in the experiment, the total number of 16 model parameters is updated at 0.1 Hz. The optimization is performed every tenth recursion of model parameters because of the time delay in the data transfer between the target PC and the host PC. The sensor weighting is hence updated at 0.01 Hz and it is fixed until a new set is computed and updated. The 16^{th} order controller is updated at 16.67 Hz while a linear model for the controller design is updated at 50 Hz. These sample rates are limited by the target PCs in the experiment. In the process of the optimization, the weighted reference sensor signal is generated from an optimal set of three sensors. Figure 7 shows the averaged open- and closed-loop auto-spectrum estimation of the PSD signal. Although spillover is observed in nearby frequencies, the jitter is reduced significantly (31 dB) at 550 Hz.

Second, the plate structure is disturbed by band-limited (2 kHz) random disturbance. The random disturbance signal is applied to one of the actuators mounted on the plate — actuator 1 in Figure 4. Figure 8 shows the averaged open- and closed-loop frequency response function (FRF) magnitude plot of the PSD signal when actuator 1 is the disturbance source (Configuration 1). The overall response is attenuated by 5.3 dB between 300 Hz and 800 Hz, and by 6.3 dB between 400 Hz and 600 Hz.

While the algorithm is running in real time, the disturbance source is switched to the other actuator — Actuator 2 in Figure 4. Actuator 2 is also excited with band-limited (2 kHz) random disturbance. Figure 9 shows the averaged open- and closed-loop FRF magnitude plot of the PSD signal when actuator 2 is the disturbance source (Configuration 2). The overall response is attenuated by 6.2 dB between 300 Hz and 800 Hz, and by 6.7 dB between 400 Hz and 600 Hz.

In order to observe the performance of the proposed sensor weighting algorithm, the adaptive generalized predictive control algorithm is applied with single disturbance measurement sensor which is one of the optimal

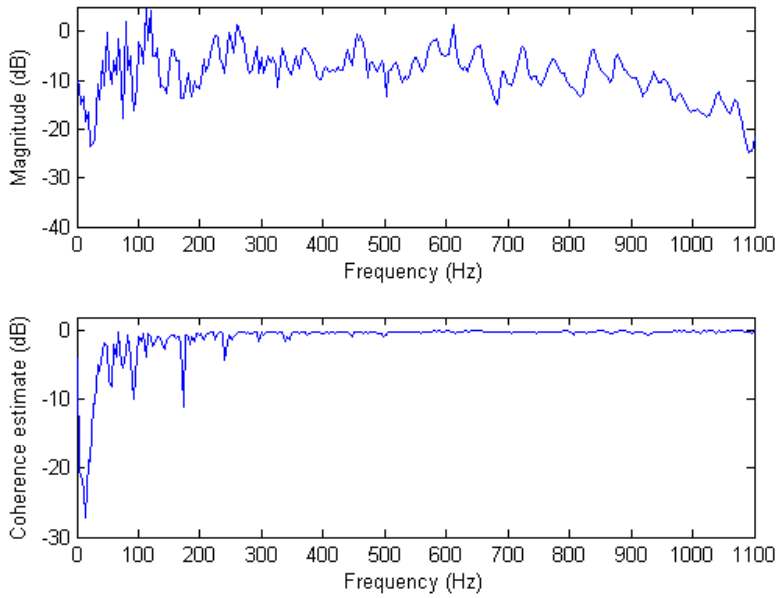

Figure 6. (a) Frequency response plot of the averaged magnitude, (b) Averaged coherence estimation plot between disturbance signal and accelerometer signals

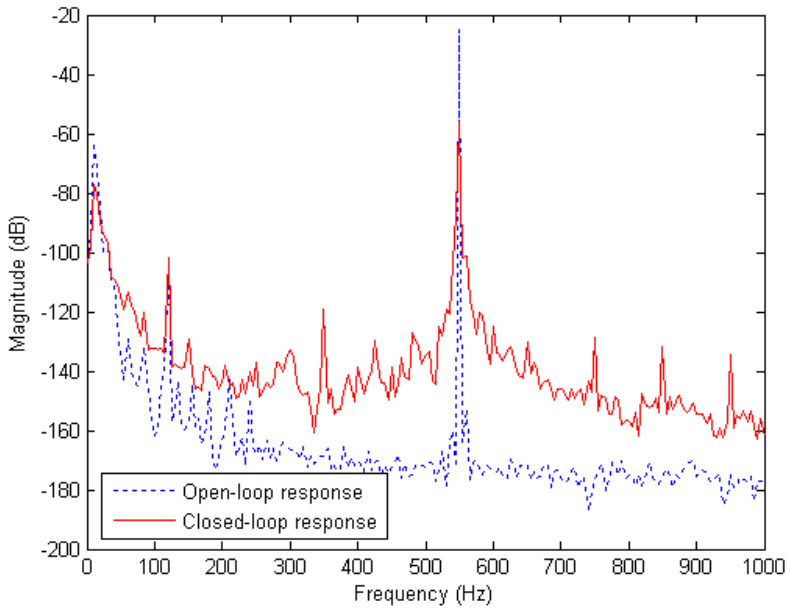

Figure 7. Auto-spectrum estimation plot of PSD signal when single frequency (550 Hz) disturbance is applied.

set observed in the previous experiments. Figure 10 shows the FRF magnitude plot for configuration 1. The response is attenuated by by 4.2 dB between 300 Hz and 800 Hz, and by 4.6 dB between 400 Hz and 600 Hz. Figure 11 shows the FRF magnitude plot for configuration 2. The response is attenuated by 4.9 dB between 300 Hz and 800 Hz, and by 5.3 dB between 400 Hz and 600 Hz.

VII. Summary

The optimal sensor weighting technique accomplished through the use of the Hankel Singular Value approximation and the genetic optimization algorithm was explored. The algorithm was then demonstrated on the optical jitter test bed with the adaptive generalized predictive control algorithm. In the jitter test bed, optical elements — a turning mirror and its mounting post — mounted on the plate structure were disturbed by the structural vibration on the plate. The adaptive control design using the weighted reference sensor signal resulted in greater jitter reduction than using a single reference sensor signal. In addition, by using the RLS algorithm to update the model parameters continuously in real time, the overall algorithm can respond to environmental/system changes.

VIII. Acknowledgments

The authors would like to thank the Air Force Research Laboratory at Kirtland Air Force Base in Albuquerque, NM and the Missile Defense Agency, contract No. FA9453-04-C-0013, for providing funding for this research.

References

[1]M. A. McEver, D. G. Cole, and R. L. Clark. Adaptive feedback control of optical jitter using Q-parameterization. *Optical Engineering*, 43(04):904–910, 2004.

[2]D. A. Kienhols. Active alignment and vibration control system for a large airborne optical system. *Proc. SPIE*, 3989:464–471, April 2000.

[3]W. B. DeShetler and J. D. Dillow. Suppression of noise in the airborne laser system. *Proc. SPIE*, 3706:249–257, 1999.

[4]M. A. McEver and R. L. Clark. Active jitter suppression of optical structures. *Proc. SPIE: Smart Structures and Materials*, 4327:591–599, 2001.

[5]S.-M. Moon, R. L. Clark, and D. G. Cole. Recursive generalized predictive control for systems with disturbance measurements. *Proc. SPIE: Smart Structures and Materials, Damping and isolation*, 5383:320–331, July 2004.

[6]F. Bondu, P. Hello, and J.-Y. Vinet. Thermal noise in mirrors of interferometric gravitational wave antennas. *Physics Letters A*, 246:227–236, 1998.

[7]R. M. Glaese, E. H. Anderson, and P. C. Janzen. Active suppression of acoustically induced jitter for the airborne laser. *Proc. SPIE*, 4034:151–164, 2000.

[8]M. W. Oppenheimer and M. Pachter. Adaptive optics for airborne platforms – Part 1: Modeling. *Optics and Laser Technology*, 34:143–158, 2002.

[9]S.-M. Moon, R. L. Clark, and D. G. Cole. The recursive generalized predictive feedback control: theory and experiments. *The Journal of Sound and Vibration*, 279:171–199, 2005.

[10]M. A. McEver, D. G. Cole, and R. L. Clark. Experiments in adaptive optical jitter control. *Proc. SPIE: Smart Structures and Materials*, 5049:275–282, 2003.

[11]M. A. Tascillo V. A. Skormin and T. E. Busch. Demonstration of a jitter rejection technique for free-space laser communication. Technical Report 2, April 1997.

[12]M. A. Tascillo V. A. Skormin and D. J. Nicholson. A jitter rejection technique in a satellite-based laser communication system. Technical Report 2, April 1993.

[13]S.-M. Moon, L. P. Fowler, and R. L. Clark. Optimal sensing strategy for adaptive control of optical system. *Proc. SPIE: Smart Structures and Materials*, To be published, 2005.

[14]B. L. Ho and R. E. Kalman. Effective construction of linear state-variable models from input/output data. *Proceedings of the 3rd Annual Allerton Conference on Circuit and System Theory*, pages 449–459, 1965.

[15]J.-N. Juang. *Applied System Identification*. Prentice-Hall, Englewood Cliffs, NJ., 1994.

[16]L. Ljung. *System Identification: Theory for the User*. Prentice Hall, Englewood Cliffs, NJ., 2nd edition, 1999.

[17]K. B. Lim, R. C. Lake, and J. Heeg. Effective selection of piezoceramic actuators for an experimental flexible wing. *AIAA Journal of guidance, Control and Dynamics*, 21(5):704–709, 1998.

[18]R. E. Richard and R. L. Clark. Computationally efficient piezostructure modeling for system optimization. *Proc. SPIE: Smart Structures and Materials*, 4701:389–400, July 2002.

[19]Gordon C. Smith. *Design Methodologies for Optimal Spatial Compensation of Adaptive Structures*. PhD thesis, Duke University, May 2000.

[20]Robert E. Richard. *Optimized Flutter Control for an Aeroelastic Delta Wing*. PhD thesis, Duke University, 2002.

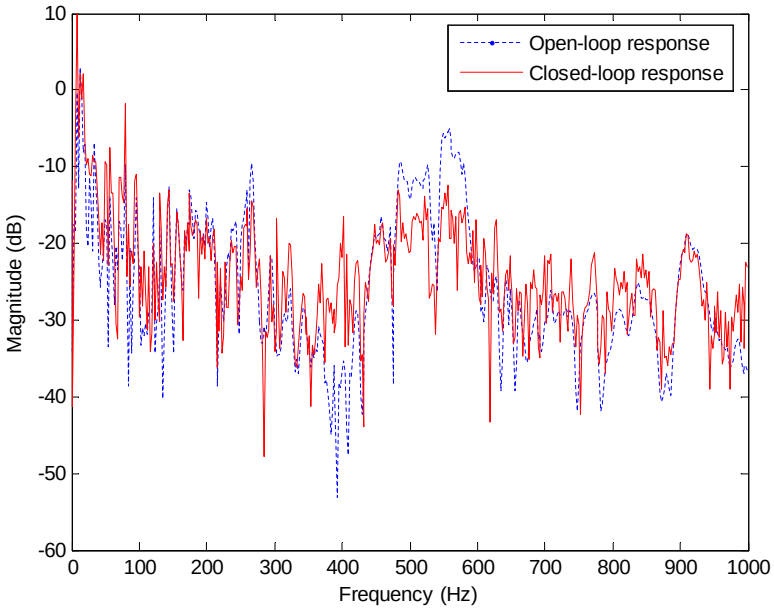

Figure 8. Frequency response function magnitude plot between disturbance signal and PSD signal using weighted disturbance signals: Configuration 1

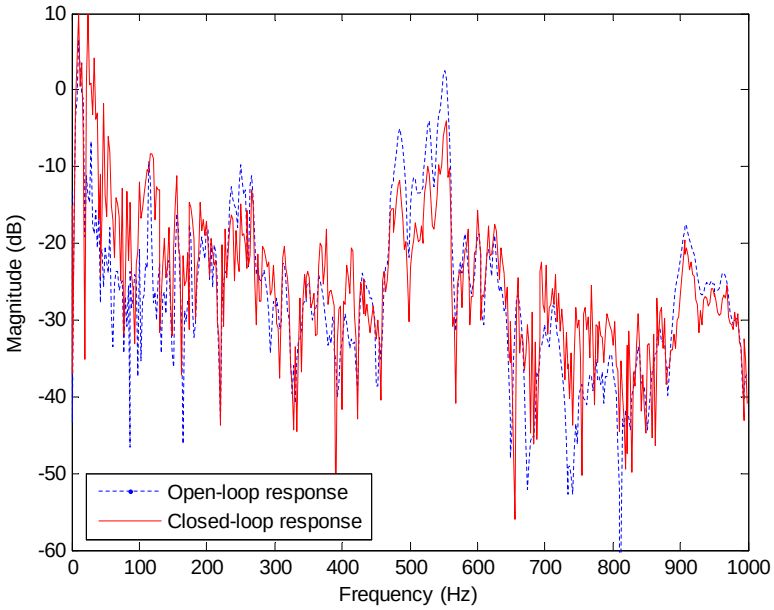

Figure 9. Frequency response function magnitude plot between disturbance signal and PSD signal using weighted disturbance signals: Configuration 2

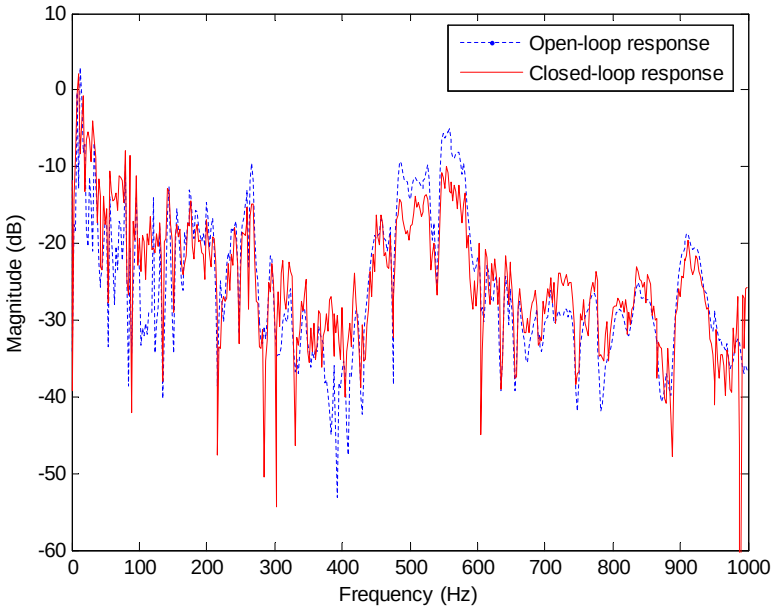

Figure 10. Frequency response function magnitude plot between disturbance signal and PSD signal using single disturbance signal: Configuration 1

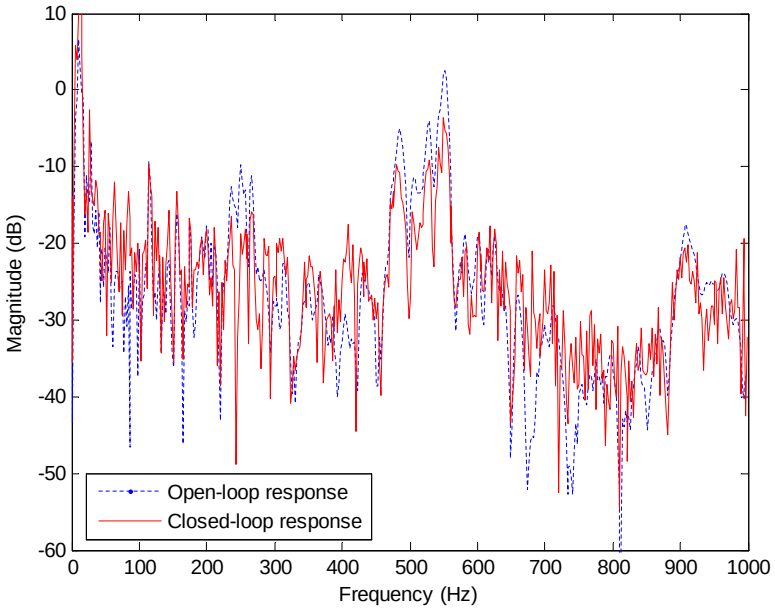

Figure 11. Frequency response function magnitude plot between disturbance signal and PSD signal using single disturbance signal: Configuration 2

[21]Suk-Min Moon. *On-line generalized predictive control combined with recursive least squares system identification*. PhD thesis, Duke University, 2003.

[22]D. W. Clarke, C. Mohtad, and P. S. Tuffs. Generalized predictive control - part I. the basic algorithm. *Automatica*, 23(2):137–148, 1987.

[23]J.-N. Juang and M. Phan. Deadbeat predictive controllers. Technical Report TM-112862, NASA, May 1997.

[24]J.-N. Junag and K. W. Eure. Predictive feedback and feedforward control for systems with unknown disturbance. Technical Report TM-208744, NASA, December 1998.

[25]S. M. Kay. *Modern Spectral Estimation*. Prentice-Hall, 1988.